

Bias-Voltage Dependence in Atomic-Scale Spin Polarized Scanning Tunneling Microscopy of Mn_3N_2 (010)

Arthur R. Smith, Rong Yang, and Haiqiang Yang

Department of Physics and Astronomy, Condensed Matter and Surface Science Program and Nanoscience and Quantum Phenomena Institute, Ohio University, Athens, OH 45701

ABSTRACT

Atomic-scale spin-polarized scanning tunneling microscopy results on the manganese nitride Mn_3N_2 (010) surface are presented. The images show the row-wise antiferromagnetic structure of the surface. It is shown that the bias voltage between tip and sample affects both the magnetic and non-magnetic components of the height profile. In particular, a reversal of the magnetic contrast is shown to occur at a certain bias voltage.

INTRODUCTION

Spin-polarized scanning tunneling microscopy (SP-STM) is a very promising technique for the study of surface magnetism since detailed magnetic contrast can be obtained down to the atomic scale [1,2,3]. Previous work done by Heinze *et al.* showed magnetic contrast for a Mn monolayer on W (110) [1]. Such a capability to study the fine detail of the spin structure is very important considering the growing interest in nanoscale magnetism as well as spintronics. Unfortunately, not enough is known about this technique. For example, little is known how the magnetic contrast varies with tunneling parameters, such as bias voltage. The surface magnetic structure of Mn_3N_2 (010) – a model row-wise antiferromagnetic surface – makes an ideal testing ground for the technique of atomic-scale SP-STM. In recent work, we have demonstrated both magnetic and non-magnetic contrast obtained simultaneously on this surface [3]. Here, we present results showing bias-dependence of the magnetic contrast amplitude, and also that the magnetic contrast reverses at a certain bias. The explanation for this behavior is discussed.

EXPERIMENTAL DETAILS

The experiments are performed in a custom molecular beam epitaxy/scanning tunneling microscopy (MBE/STM) ultra-high vacuum system. The sample of Mn_3N_2 (010) is prepared by MBE using a Mn effusion cell and a radio frequency (rf) plasma N source. The substrate used is MgO(001). The grown sample is transferred directly into the adjoining STM chamber without air exposure for the SP-STM study. The tips for SP-STM are prepared in various ways, typically by coating outgassed W tips with a 5-10 monolayer Mn or Fe film. In the case of Fe coatings, a small magnetic field is also applied normal to the tip axis following deposition. The SP-STM experiments are performed at room temperature in constant current mode.

DISCUSSION

The principle of SP-STM is based not on the magnetic force between the tip and the sample, but rather on the existence of a spin-polarized local density of states (LDOS) for the tip and also for the sample. Shown in Figure 1 is a schematic diagram illustrating the basic concept of the

atomic-scale SP-STM method. In this method, a magnetic-coated tip scans a magnetic surface, here depicted as an antiferromagnetic surface in which the spins of the atoms alternate in direction from one atom to the next. The expected line profile is composed of the normal atomic height profile (non-magnetic part of the profile) modulated by the magnetic component. As can be seen, where the tip and sample spins are parallel, the higher peak occurs, and where they are antiparallel, the lower peak occurs. If the tip or sample (or both) is non-spin-polarized, the peaks will all have the same height, equal to the average height of the modulated peaks. It is important to realize that both magnetic and non-

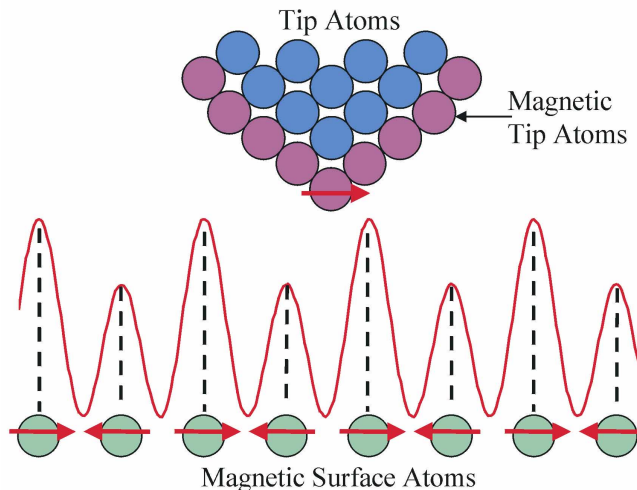


Figure 1. Schematic illustration of the SP-STM method. The tunneling current and thus the height depends on the relative orientations between tip and sample spins.

magnetic components are electronic in origin, the magnetic one being related to an imbalance in the spin- \uparrow LDOS and spin- \downarrow LDOS. To understand the contrast mechanism, it should be realized that the tunneling current is related to the product of the non spin-polarized LDOS of tip and sample (n_T and n_S) plus the vector dot product of the spin-polarized LDOS of tip and sample (\mathbf{m}_T and \mathbf{m}_S). For either tip or sample, the non spin-polarized LDOS n is just the sum of up and down spin channels ($n_\uparrow + n_\downarrow$) while the magnitude of the spin-polarized LDOS m is the difference of these two ($n_\uparrow - n_\downarrow$). Thus the height of the tip follows the formula [2,3,4]:

$$z \sim \Delta I_t(\mathbf{R}_T, V, \theta) \sim \int n_T n_S(\mathbf{R}_T, V) + \int \mathbf{m}_T \mathbf{m}_S(\mathbf{R}_T, V) \cos\theta - \text{Constant} \quad (1)$$

When m_T or m_S is zero (which implies $n_\uparrow = n_\downarrow$), the spin-polarized term goes to zero and the line profile just corresponds to the non-magnetic component. Also, if the angle θ between \mathbf{m}_T and \mathbf{m}_S is 90° , the spin-polarized term goes to zero. But if these conditions are not true, then a spin-polarized component will exist.

The ideal testing ground to observe the effects of a spin-polarized component of the tunneling current is therefore an antiferromagnetic system in which the spin directions alternate from atom to atom or from row to row. Mn_3N_2 (010) is such an ideal surface. Normal atomic-resolution images of this surface reveal the structure, as shown in Figure 2 [5]. As can be seen, the surface is composed of rows of Mn atoms in a face-centered tetragonal structure. Two species of Mn atoms are resolved – Mn1 and Mn2. They arise from the 3:2 ratio of Mn:N. In every third row (and atomic layer perpendicular to the surface) there are no N atoms. Therefore the “bright” atoms (Mn1) correspond to Mn atoms in layers without N, while the less bright atoms (Mn2) correspond to Mn atoms in layers with N. The N atoms do not appear since their density of states at the Fermi level is small in comparison with that of the Mn atoms [6]. The detailed model of the bulk and surface have been discussed in detail elsewhere; therefore, the atomic structure of the surface is very well known [5,7]. As can be seen in the surface model, the spin of the Mn atoms is aligned ferromagnetically along the [100] surface direction but alternates along the [001] surface direction. The lattice constant $a = 4.21 \text{ \AA}$, while the spacing

between Mn1 rows $c/2 = 6.07 \text{ \AA}$. This structure therefore leads to a magnetic period equal to $c = 12.14 \text{ \AA}$.

Study of the Mn_3N_2 (010) surface with magnetic-coated STM tips results in images like that shown in Figure 3. This image was acquired using a Mn-coated W tip. It shows three separate terraces separated by two atomic height steps. The step height equals $a/2 = 2.1 \text{ \AA}$. The step edge appears bright due to a local background subtraction used to display all three terraces. What is observed on each terrace is the row structure, where each row corresponds to one Mn1 and two Mn2 single atomic rows. The rows are therefore separated by the Mn1 layer spacing = $c/2 = 6.07 \text{ \AA}$. The individual Mn atoms are not resolved in the image. However, what is observed is that the height of the observed rows is modulated, and the period of the modulation corresponds to the magnetic period = c . Considering the model of the surface shown in Figure 2(b), the direction of the Mn1 spins alternates from one Mn1 row to

the next Mn1 row; that alternation is indicated in Figure 3 by the alternating direction of the arrows. It can be noted that the alternation of the spin is not interrupted by the step edges. It is concluded therefore that the image reveals the atomic-scale spin structure of the surface. In particular it corresponds to the alternation of the Mn1 spin direction every $c/2 = 6.07 \text{ \AA}$ (magnetic period = c).

Also on the terraces one observed numerous small defects which are most likely Mn atom vacancies. These defects clearly do not affect the long range magnetic order of the antiferromagnetic surface. This is again consistent with the point that the spins are ferromagnetic in bulk planes, those planes being perpendicular to the surface, and

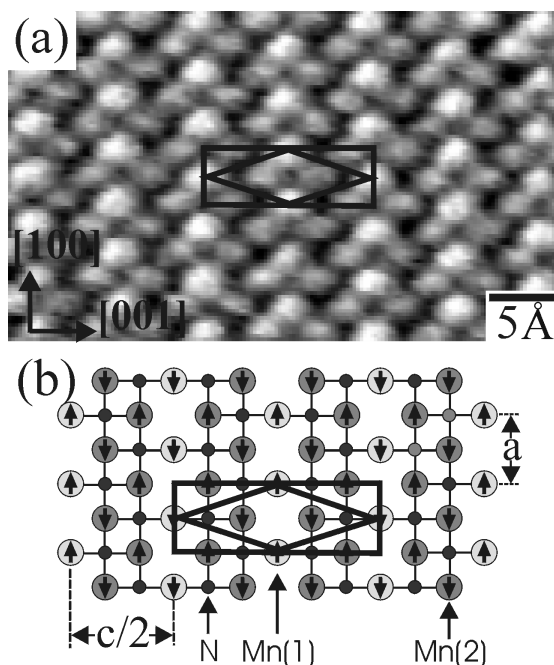


Figure 2. (a) Atomic resolution STM image of Mn_3N_2 (010) acquired with a non-magnetic STM tip; (b) atomic model of the surface showing the magnetic unit cell (rectangular) and non-magnetic unit cell (diamond shape).

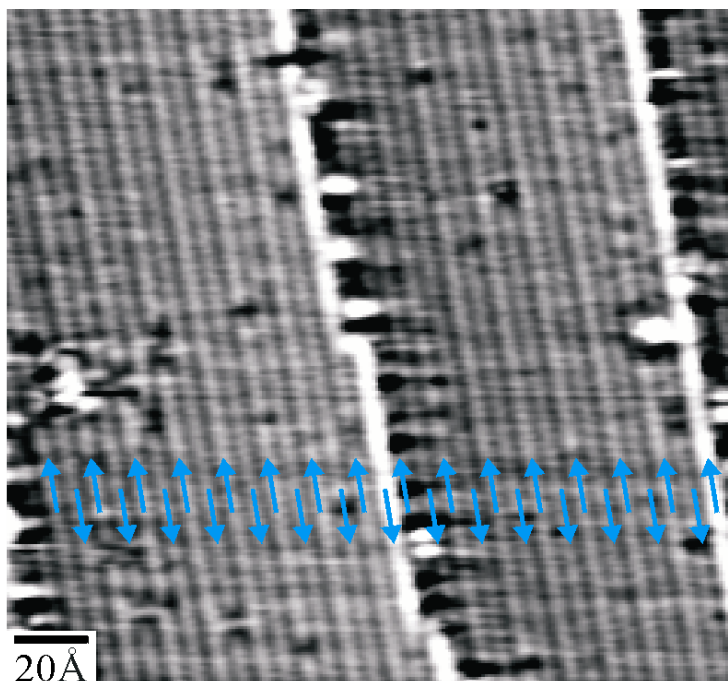


Figure 3. SP-STM image of Mn_3N_2 (010) surface obtained with Mn-coated W tip. Image was acquired with sample bias $V_s = -0.2 \text{ V}$ and tunneling current $I_t = 0.3 \text{ nA}$. Step edge brightening is due to a local background subtraction used to display the image.

that the spins in bulk alternate as a layer-wise antiferromagnet along the [001] direction (normal to the [100] row direction). Since the surface spin directions are determined by the bulk spin directions, the magnetic modulation in the image follows the same periodicity.

The same SP-STM experiment is performed at various sample biases, as shown in Figure 4. These four images were acquired using a Fe-coated W tip from the exact same location on the sample surface which was determined using several surface defects as reference points (not included in the images). Several interesting points can be made from these four images. First of all, the gray scale magnetic contrast is seen at all four bias voltages (+0.6 V, +0.2 V, -0.2 V, and -0.6 V); this is seen as an alternation of the apparent brightness of the rows. The magnetic contrast is yet better depicted in the line profiles averaged over the vertical direction shown below each image. In the line profiles, one can see that both the non-magnetic as well as the magnetic contrast is observed. The non-magnetic contrast is the main part of the line profile having period equal to the row spacing $c/2$ (the distance between each adjacent peak, or each row of Mn1 atoms). The magnetic contrast is the modulation of the peak height, a component having a period of c (the magnetic period) or twice that of the row spacing.

What is also clear is that the magnetic contrast reverses over the range between +0.6 V and +0.2 V. This is seen as the 3 high peaks at +0.6 V become the 3 low peaks at +0.2 V, and the 2 low peaks at +0.6 V become the 2 high peaks at +0.2 V. The same polarity of the magnetic contrast as at +0.2 V is maintained as the bias is further decreased to -0.2 V and -0.6 V. Thus a single magnetic contrast reversal is observed over this voltage range, and furthermore, the point of reversal is not at 0 V. Rather, the reversal occurs at about +0.4 V.

Polarity reversal can be understood by the energy-dependent spin-polarized LDOS of the tip and that of the sample. In order to obtain magnetic contrast reversal, it is necessary that the magnetic term in the tunneling current $\int \mathbf{m}_T \cdot \mathbf{m}_S$ changes sign with the voltage. This can occur in several ways. It must be realized that the surface magnetic moments (as well as the tip magnetic moments) are fixed quantities (in both magnitude and direction), determined for a given atom by the integral over all its filled magnetic states. Application of different bias voltage does not affect the magnetic moments. However, SP-STM is sensitive not to the entire magnetic moment, but only to the magnetic LDOS integrated over the small energy range from the E_F to $E_F + eV_S$; therefore, it is possible (even likely) for the sample integrated magnetic LDOS to change sign at a certain bias. It is also possible for the tip magnetic LDOS to change

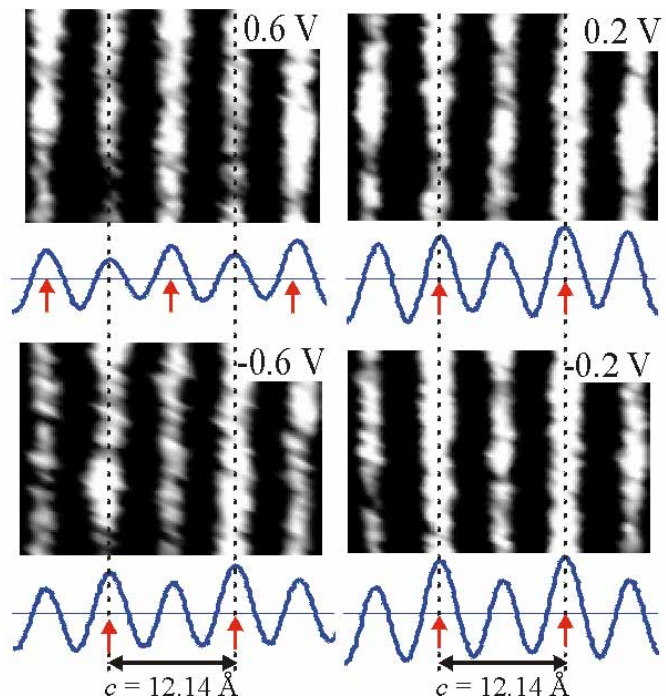


Figure 4. SP-STM images of Mn_3N_2 (010) as a function of the sample bias. In each case, the tunneling current was 0.3 nA. Vertical arrows indicate the high peak position.

sign at a certain bias. More detailed discussion for the contrast reversal shown here will be given elsewhere [8].

SP-STM images of the same local area as shown in the data of Figure 4 were taken, and the average line profiles for each image were determined. In order to examine how the magnetic and non-magnetic components of the data each vary independently with the sample bias, it is important to separate these two components. A separation procedure has been developed [3] and follows from the symmetry and periodicity of the surface structure. The resulting equations are as follows:

$$\int m_T m_S(x) \cos[\theta(x)] \sim [z(x) - z(x+c/2)]/2 \quad (\text{magnetic component}) \quad (2)$$

$$\int n_T n_S(x) \sim [z(x) + z(x+c/2)]/2 + C \quad (\text{non-magnetic component}) \quad (3)$$

These two separated profiles are obtained from each total line profile. An example of the separation of magnetic and non-magnetic height profiles is shown in Figure 5. As can be seen, the magnetic profile has twice the period of the non-magnetic profile and only a fraction of the amplitude.

The amplitudes (in Å) of the magnetic and non-magnetic profiles are then obtained for each sample bias. The results are presented in Figure 6. The amplitude data points are shown together with a smooth fitted curve. As can be seen, the amplitude of both components varies considerably with the bias voltage. The deduced non-magnetic amplitude vs. bias behavior is in very good agreement with similar data based on atomic resolution images acquired with a non-magnetic probe tip [9]. The non-magnetic amplitude is largest at +0.1 V, although the maximum of the smoothed curve is at slightly negative bias. The magnetic amplitude is maximum at about -0.1 V and decreases for further negative bias. It also decreases more steeply for positive bias, going through zero at +0.4 V. This is the point of magnetic contrast reversal. At larger positive voltages, the amplitude increases again but with the opposite sign.

CONCLUSIONS

It has been shown that magnetic and non-magnetic contrast is obtained at the atomic scale using SP-STM for the case of Mn_3N_2 (010). Reversal of the magnetic contrast occurs at a positive sample bias voltage, indicating a reversal in the sign of $\int \mathbf{m}_T \cdot \mathbf{m}_S$, the magnetic component of the tunneling current. Furthermore, the amplitudes of the magnetic and non-magnetic components of the height profile have been shown to be maximized near the

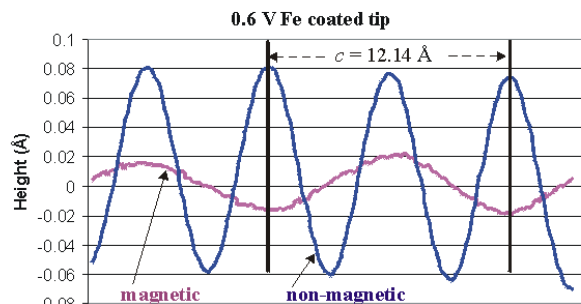


Figure 5. Plot of the separated magnetic and non-magnetic height profiles obtained at sample bias +0.6 V.

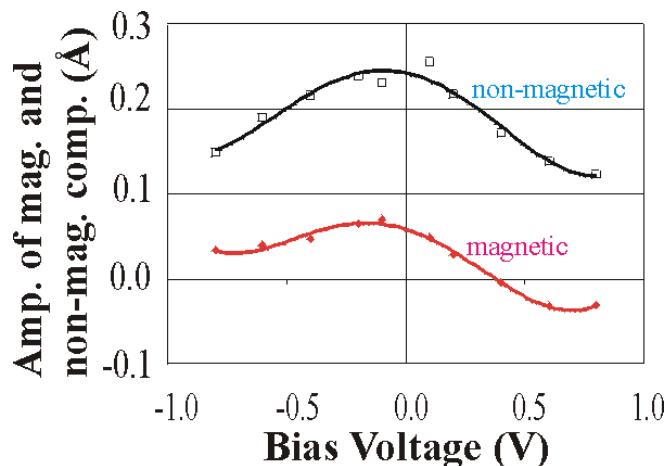


Figure 6. Amplitude of magnetic and non-magnetic corrugations observed in the SP-STM experiments as a function of the sample bias voltage.

Fermi level for Mn_3N_2 (010). The present study shows that the magnetic contrast obtained with SP-STM is very sensitive to the tunneling parameters, in particular the bias voltage, which is important for future measurements of nanometer-scale magnetic systems using this technique.

ACKNOWLEDGEMENTS

The authors thank the National Science Foundation under Grant numbers 9983816 and 0304314. Also, the authors acknowledge prior support by the Office of Naval Research and the continual support of Ohio University.

REFERENCES

1. S. Heinze, M. Bode, A. Kubetzka, O. Pietzsch, X. Nie, S. Blügel, and R. Wiesendanger, *Science* **288**, 1805 (2000).
2. D. Wortmann, S. Heinze, Ph. Kurz, G. Bihlmayer, and S. Blügel, *Phys. Rev. Lett.* **86**, 4132 (2001).
3. H. Yang, A.R. Smith, M. Prikhodko, W.R.L. Lambrecht, *Phys. Rev. Lett.* **89**, 226101 (2002).
4. A. R. Smith, R. Yang, H. Yang, and W.R.L. Lambrecht, to be published.
5. H. Yang, H. Al-Britthen, A. R. Smith, J.A. Borchers, R.L. Cappelletti, and M.D. Vaudin, *Appl. Phys. Lett.* **78**, 3860 (2001).
6. W.R.L. Lambrecht, M. Prikhodko, and M. S. Miao, *Phys. Rev. B* **68**, 174411 (2003).
7. G. Kreiner and H. Jacobs, *J. Alloys and compounds* **183**, 345 (1992).
8. R. Yang, H. Yang, A. R. Smith, *et al.* to be published.
9. H. Yang, R. Yang, A. R. Smith, and W.R.L. Lambrecht, *Surface Science* **548**, 117 (2004).